J. Meseguer, A. Sanz, J. M. Perales

Axisymmetric Long Liquid Bridges Stability and Resonances

In this paper mathematical expressions for minimum-volume stability limits and resonance frequencies of axisymmetric long liquid bridges are presented. These expressions are valid for a wide range of liquid bridge configurations, accounting for effects like unequal disks and axial microgravity in the case of minimum-volume stability limits, and unequal disks, axial microgravity, non-zero viscosity and liquid bridge volume different from the cylindrical one in the case of resonance frequencies.

1 Introduction

Floating zones appear in a large variety of industrial processes in which the handling of non-confined liquids is required. A typical example of these processes is the so-called floating zone melting technique [1] which is used in crystal growth and in purification of high melting point materials [2]. As it is well-known, in a ground laboratory the maximum stable length of a vertically suspended liquid zone is limited by the balance between the hydrostatic pressure (which increases with the distance to the top of the liquid zone) and the capillary forces; this constraint can be partially removed by working in a reduced-gravity environment like a space platform (rendering liquid zones more accessible than on earth). Thus, there is an increasing interest, from both commercial and scientific points of view, in the use of space platforms for materials processing. In fact, several attempts have been made in the past dealing with floating zones in space [3, 4].

The study of liquid zones involves a large effort both because of the material characteristics of the melt (whose properties are temperature-dependent) and because of the complexities associated with the geometrical configuration and with the disturbances that may be imposed on the liquid zone. Thus, depending on the formulation of the liquid zone problem under study, different simplifications may be introduced in the model. In this sense, when the aim is to analyze the mechanical behaviour of the liquid zone, the simplest approach is to disregard thermal effects, considering the liquid zone as a mass of liquid, with uniform and constant properties, held by capillary forces between two parallel, coaxial, solid disks (fig. 1). This idealization of the floating zone problem is known as the liquid bridge problem.

Liquid bridges have drawn the attention of numerous scientists during the last fifteen years, and considerable efforts have been devoted, and are being devoted, to study such a fluid configuration, either from a theoretical or an experimental point of view. Leaving apart experimental research on ground laboratories, several experiments concerning liquid bridges have been performed aboard Spacelab-1 [5], Spacelab-D1 [6], and TEXUS sounding rockets [7], and new experiments dealing with such fluid configurations are scheduled to be carried out aboard TEXUS and Spacelab-D2. From the theoretical point of view, there is a large background concerning liquid bridges (a short review of the state of the art in this field can be found in [8]). However, most of the information is only available as numerical or graphical information, except for some particular liquid bridge configurations which have been analyzed through simplified models where useful, although very limited in range, analytical expressions (mainly for equilibrium shapes and stability limits) are available [9, 10, 11, 12].

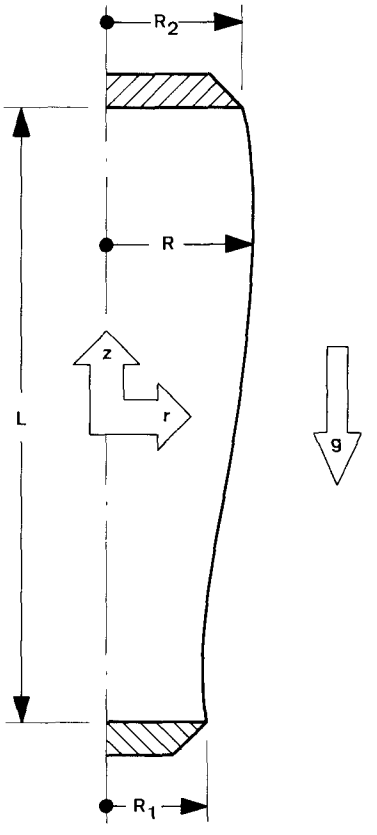

Fig. 1. Geometry and cordinate system for the liquid bridge problem

In this paper mathematical expressions for both the minimum-volume stability limit and the resonance frequencies corresponding to the first mode of axisymmetric liquid bridges between unequal disks subjected to an axial microgravity field are presented. These expressions have been obtained by fitting suitable mathematical expressions to available data, and are valid in a wide range of values of the liquid bridge slenderness, $2 \leq \Lambda \leq 3.2$ (where $\Lambda = L/(R_1 + R_2)$, L being the liquid bridge length and R_1 and R_2 the radius of the disks), disks radius ratio, $0.8 \leq K \leq 1$ (where $K = R_1/R_2$) and Bond number, $|B| \leq 0.1$ in the case of stability limits and $|B| \leq 0.05$, at least, in the case of resonance frequencies (where $B = \varrho g R_0^2/\sigma$, ϱ being the liquid density, g the microgravity acceleration, σ the surface tension and $R_0 = (R_1 + R_2)/2$ the mean radius).

2 Minimum Volume Stability Limit

The dimensionless minimum-volume stability limit, V_m, is the minimum volume of liquid for which the liquid configuration remains stable, that is, if the volume of liquid diminishes below V_m the fluid configuration becomes unstable, and the breaking of the liquid column takes place. The minimum-volume stability limit depends on Λ, K, and B, although analytical [13], numerical [14], and experimental [11] results seem to indicate that B and K (both are non-symmetric effects with respect to the middle plane parallel to the disks) may be grouped in a new parameter accounting for both effects simultaneously, at least for liquid bridges having cylindrical volume, $V = 2\pi\Lambda$, and $\Lambda \approx \pi$. For instance, the following expression for V_m presented in [10][1]

$$V_m = 2\Lambda(2\Lambda - \pi) + 6(3/2)^{1/3}\pi\Lambda[B - H/(2\Lambda - 2\sin\Lambda)]^{2/3}, \tag{1}$$

where $H = (1 - K)/(1 + K)$, states that the parameter to be considered is $D = |B - H/(2\Lambda - 2\sin\Lambda)|$ instead of B or H each separately. Equ. (1) is only valid in a small region close to the stability limit ($\Lambda = \pi$) of cylindrical volume liquid bridges, and far from this region (1) gives unacceptable errors [10]. Since a similar behaviour can be deduced from the experimental results presented in [11], aiming at getting a better approximation for V_m, the first step has been to obtain a better approximation for the parameter D, and the following new expression for D has been obtained by fitting to those experimental data

$$D = |B(49.953 - 48.197\Lambda + 12.288\Lambda^2)/(2\Lambda - \sin\Lambda) - H|. \tag{2}$$

The next step has been to fit appropriate expressions for V_m to numerical data reported in [8] concerning the influence of B on V_m, to those reported in [15] concerning the influence of K on V_m, and to those reported in [14] concerning the influence of both B and K on V_m. Different attempts have been made aiming at getting an expression for $V_m(\Lambda, K, B)$ valid for a wide range of values of Λ, K and B, and the more accurate one found is

$$V_m = 2\pi\Lambda + (C_0 + C_1\Lambda)\Lambda^N, \tag{3}$$

where

$$\left.\begin{aligned} C_0 &= -3.4329 - 6.1954 D^{3/4} + 10.0737 D^{3/2} \\ C_1 &= 1.0947 + 3.1683 D^{3/4} - 1.2156 D^{3/2} \\ N &= 2.1291 - 0.7504 D^{3/4} + 0.8771 D^{3/2} \end{aligned}\right\} \tag{4}$$

Eq. (3) gives V_m with an error smaller than 1% (in the range $2 \leq \Lambda \leq 3.2$, $0.5 \leq K \leq 1$) when compared with numerical results reported in [15], and an error similar or even smaller when compared with numerical results reported in [8, 14].

The variation of V_m with Λ and B, eq. (3), is shown in fig. 2 for the case of equal disks ($K = 1$) and in fig. 3 in the case of unequal disks ($K = 0.8$). Note that in these plots the curves corresponding to $|B| > 0.1$ are out of the validity range of eq. (3).

3 Dynamic Response of Liquid Bridges in a Time-Dependent Microgravity Field

In a previous paper [16] a numerical method to calculate the dynamic response, hence the frequencies of resonance, of long inviscid liquid bridges between unequal disks in a time-dependent axial microgravity field was presented. That method has been used here to obtain the dimensionless resonance pulsation (corresponding to the first mode) of a reasonable number of liquid bridge configurations; these values of the resonance pulsation, ω_r, are used to fit a mathematical expression for ω_r which accounts for the effect on ω_r of Λ, B, K and the dimensionless liquid bridge volume, V. However, as a previous step before presenting the resulting expression for ω_r, let us introduce two simple linear one-dimensional models from which it is possible to obtain analytical expressions for the dynamic response of liquid bridges in a time-dependent microgravity field. The first model is the particular case of the general formulation reported in [16] in which the disks are both equal ($K = 1$) and the liquid bridge volume is the cylindrical one ($V = 2\pi\Lambda$). The second model is derived from the formulation for the liquid bridge dynamics presented in [17] and, although it is valid only for liquid bridge slendernesses close to $\Lambda = \pi$, allows one to analyze the influence on ω_r of liquid bridge volumes other than the cylindrical one, of a mean level of microgravity different from zero, and also the influence of the liquid viscosity.

3.1 One-Dimensional Inviscid Slice Model

Let us consider a slender liquid bridge held by surface tension forces between two equal disks ($R_1 = R_2 = R_0$). If the liquid bridge volume is the cylindrical one, $V = 2\pi\Lambda$, under gravitationless conditions the dimensionless equation of the liquid-gas interface at rest will be $S(z) = R^2(z) = 1$. If the microgravity is assumed to be time-dependent, $\varepsilon g(t)$, where $\varepsilon \ll 1$ stands for the order of magnitude, such time dependence will affect the shape of the liquid bridge interface in such a way that the actual shape could be expressed as $S(z, t) = 1 + \varepsilon\bar{s}(z, t)$. Then, under the assumptions stated in [16] the problem formulation becomes

Continuity equation

$$S_t + Q_z = 0. \tag{5}$$

1 There is an error in all the expressions for V_m in [10]: the correct factor is $(3/2)^{1/3}$ instead of the value $(3/2)^{4/3}$ appearing in that paper.

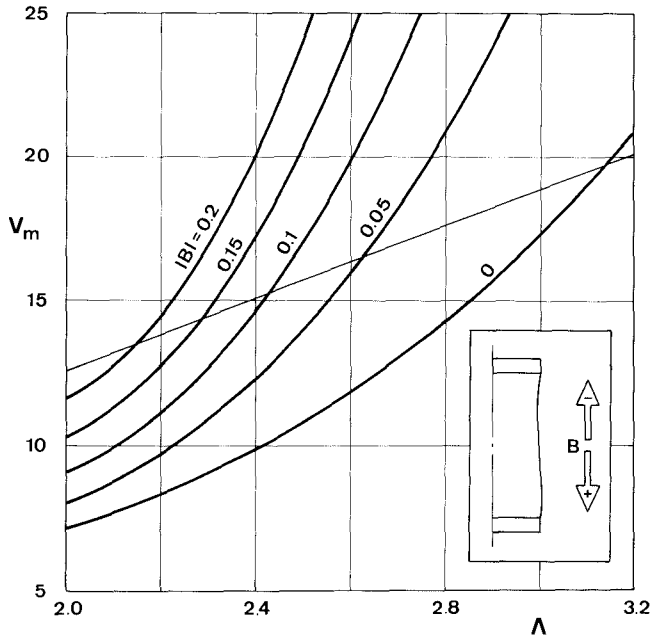

Fig. 2. Variation with the slenderness Λ and the Bond number B of the minimum volume stability limit V_m of axisymmetric liquid bridges between equal disks (disks radius ratio $K = 1$). The thin straight line corresponds to liquid bridges having cylindrical volume ($V = 2\pi\Lambda$)

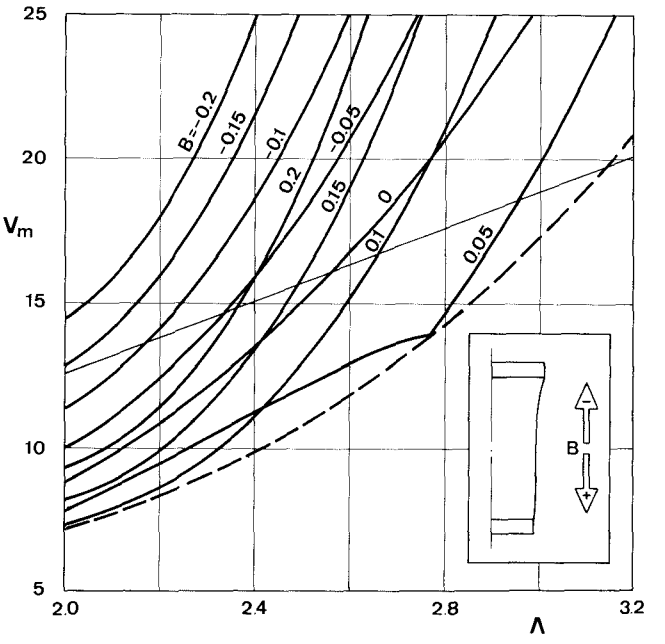

Fig. 3. Variation with the slenderness Λ and the Bond number B of the minimum volume stability limit V_m of axisymmetric liquid bridges between unequal disks (disks radius ratio $K = 0.8$). The thin straight line corresponds to liquid bridges having cylindrical volume ($V = 2\pi\Lambda$) whereas the dashed line corresponds to the absolute minimum volume stability limit

Axial momentum equation

$$Q_t + (Q^2/S)_z = -SP_z, \tag{6}$$

where $Q = SW$, W being the axial velocity which is assumed to be constant at each slice parallel to the disks, and

$$P = 4[4S + (S_z)^2]^{-3/2}[2S + (S_z)^2 - SS_{zz}] + Bz \tag{7}$$

where $B(t) = \varepsilon \varrho\, g(t)\, R_0^2/\sigma = \varepsilon\, \tilde{b}(t)$.

Boundary conditions

$$S(\pm\Lambda, t) = 1, \quad Q(\pm\Lambda, t) = 0 \tag{8}$$

Then, the introduction of the asymptotic expansions $Q(z, t) = \varepsilon\tilde{q}(z, t)$ and $P(z, t) = 1 + \varepsilon\tilde{p}(z, t)$, in addition to those stated for $S(z, t)$ and $B(t)$, in the problem formulation yields the following linearized problem

$$\tilde{s}_t + \tilde{q}_z = 0 \tag{9}$$

$$\tilde{q}_t = \frac{1}{2}(\tilde{s}_z + \tilde{s}_{zzz}) - \tilde{b} \tag{10}$$

$$\tilde{s}(\pm\Lambda, t) = 0, \quad \tilde{q}(\pm\Lambda, t) = 0 \tag{11}$$

Elimination of $\tilde{s}$ between (9) and (10) gives

$$2\tilde{q}_{tt} + \tilde{q}_{zz} + \tilde{q}_{zzzz} + 2\tilde{b}_t = 0 \tag{12}$$

$$\tilde{q}(\pm\Lambda, t) = 0, \quad \tilde{q}_z(\pm\Lambda, t) = 0 \tag{13}$$

where the second of (13) results from $\tilde{s}(\pm\Lambda, t) = 0$, taking into account the continuity equation (9).

Assuming that the Bond number varies with time sinusoidally, that is, $\tilde{b} = b\sin\omega t$, equ. (12) suggests to look for $\tilde{q}(z, t)$ solutions of the form $q(z, t) = q(z)\cos\omega t$. Therefore, after substituting these expressions in (12), and eliminating time dependent factors, finally results

$$q_{zzzz} + q_{zz} - 2\omega^2 q + 2b\omega = 0 \tag{14}$$

$$q(\pm\Lambda) = 0, \quad q_z(\pm\Lambda) = 0 \tag{15}$$

The solution of (14) is

$$q = \frac{b}{\omega} + C_1 e^{az} + C_2 e^{-az} + C_3\cos dz + C_4\sin dz \tag{16}$$

where a and d are related to ω through

$$\left.\begin{aligned} a &= \left\{\frac{1}{2}[(1 + 8\omega^2)^{1/2} - 1]\right\}^{1/2} \\ d &= \left\{\frac{1}{2}[(1 + 8\omega^2)^{1/2} + 1]\right\}^{1/2} \end{aligned}\right\} \tag{17}$$

Application of the four boundary conditions (15) to (16) gives a system of four algebraic equations which allow one to calculate the four constants C_i, the resulting expression for $q(z)$ being

$$q = \frac{b}{\omega}\left(1 - \frac{f(\omega, z)}{f(\omega, \Lambda)}\right) \tag{18}$$

where

$$f(\omega, z) = d\cosh az\sin d\Lambda + a\sinh a\Lambda\cos dz \tag{19}$$

Once $q(z)$, hence $\tilde{q}(z,t)$, is known, $\tilde{s}(z,t)$ results from the continuity equation (9), $\tilde{s}_t = -\tilde{q}_z$, and taking into account that $ad = \sqrt{2}\ \omega$, one obtains $\tilde{s}(z,t) = s(z) \sin \omega t$, where

$$s(z) = \sqrt{2}\ \frac{b}{\omega f(\omega, \Lambda)} (\sinh az \sin d\Lambda - \sinh a\Lambda \sin dz) \tag{20}$$

Equ. (20) gives the dynamic response of cylindrical liquid bridges between equal disks. The transfer function, defined as the ratio of half the maximum cross-section interface deformation to the perturbation amplitude

$$F(\omega) = s_{max}/b \tag{21}$$

can be easily obtained from (20), and the resonance pulsations are those values of ω for which $f(\omega, \Lambda)$ vanishes, that is

$$d \cosh a\Lambda \sin d\Lambda + a \sinh a\Lambda \cos d\Lambda = 0 \tag{22}$$

It must be pointed out that (22) only gives the resonance pulsations corresponding to odd modes. That means that a non-symmetric (with respect to the middle plane parallel to the disks) perturbation, like the time-dependent axial microgravity field considered above, generates only non-symmetric interface deformations (an expression giving ω_r for both odd and even modes of resonance can be found in [18], p. 130). Another feature to be pointed out is that when $\omega \to 0$ equ. (20) reproduces the static behaviour; in effect, $\omega \to 0$ means $a \to \sqrt{2}\ \omega$ and $b \to 1$, therefore $\sinh ax \to \sqrt{2}\ \omega x$, $\cosh ax \to 1$ and, then, leaving apart ω^2 terms, $s(z) = 2\ b\ (z - \Lambda \sin z/\sin \Lambda)$, which is the result obtained in [19] for the static problem.

3.2 Self-Similar, One-Dimensional Viscous Cosserat Model

The dynamics of almost cylindrical viscous liquid bridges between equal disks ($K = 1$), with slendernesses close to the value $\Lambda = \pi$, was performed in [17] by using a one-dimensional model based in a continuum Cosserat model previously used in capillary jets theory [20, 21, 22]. It is demonstrated in [17] that the dynamic behaviour of long liquid bridges can be explained by using the following self-similar variables and parameters

$$\left.\begin{aligned} \tilde{\alpha} &= \frac{1}{4} A (\lambda/3)^{-1/2} \\ \theta &= \frac{2}{5} t (2\lambda)^{1/2} \\ \gamma &= \frac{5}{2} C (2\lambda)^{-1/2} \\ \tilde{\beta} &= \frac{1}{2} B \lambda^{-1} (\lambda/3)^{-1/2} \end{aligned}\right\} \tag{23}$$

In these expressions A stands for the amplitude of a perturbation in the liquid-gas interface as $S(z,t) = 1 + A(t) \sin(\pi z/\Lambda)$, λ is a reduced slenderness which includes volume effects

$$\lambda = 1 - \frac{\Lambda}{\pi} + \frac{1}{2}\left(\frac{V}{2\pi\Lambda} - 1\right), \tag{24}$$

t is the dimensionless time, $C = \nu (\varrho/\sigma R_0)^{1/2}$ measures the ratio of viscous to capillary forces, and B stands for the Bond number, already defined.

With this choice, assuming A, λ, C, and B to be small enough, the dynamic behaviour of the liquid bridge is described by eq. (3.27) of the above-mentioned paper [17]

$$\tilde{\alpha}_{\theta\theta} + \gamma \tilde{\alpha}_\theta + \tilde{\alpha} - \tilde{\alpha}^3 + \tilde{\beta} = 0 \tag{25}$$

where the subscript θ indicates derivatives with respect to the self-similar time θ. Eq. (25) is a non-linear equation which includes both viscosity and gravity effects (in the following, $\tilde{\alpha}$, θ, γ and $\tilde{\beta}$ will be denoted with labels indicating their main physical meaning: interface deformation, time, viscosity and gravity, respectively). Eq. (25) is the well-known Duffing equation, which has been extensively analyzed, [23]. Although (25) can be easily integrated numerically, useful mathematical expressions for the transfer function $F(\omega)$ and resonance pulsation ω_r can be obtained by adding some simplifying hypotheses. In effect, let us assume that gravity is a time-dependent function like

$$\tilde{\beta} = \beta_0 + \varepsilon\beta \cos(\Omega\theta - \varphi) \tag{26}$$

where β_0 is the mean value of gravity, $\varepsilon \ll 1$ gives the order of magnitude of the perturbation, Ω is the self-similar pulsation ($\Omega = 5/2\ \omega(2\delta)^{-1/2}$ and φ stands for the difference in phase between the impressed perturbation and the interface movement. According to (26) the dependence with time of the liquid bridge interface could be written as

$$\tilde{\alpha} = \alpha_0 + \varepsilon\alpha \cos \Omega\theta \tag{27}$$

After introducing (26) and (27) in (25), one obtains the following set of problems

Zeroth order problem

$$\alpha_0 - \alpha_0^3 + \beta_0 = 0 \tag{28}$$

ε-order problem

$$(1 - 3\alpha_0^2 - \Omega^2)\alpha + \beta \cos\varphi = 0 \tag{29}$$

$$-\gamma\Omega\alpha + \beta \sin\varphi = 0 \tag{30}$$

Eqn. (28) gives the equilibrium interface shape α_0 which corresponds to a given mean perturbation β_0. As already demonstrated in [17] through a phase-plane analysis of (25) if $|\beta_0| \geq 2/\sqrt{27}$ the static liquid bridge configuration becomes unstable (eq. (28) has only one real root) whereas if $|\beta_0| < 2/\sqrt{27}$ there are three real roots in eq. (28), $\alpha_{01} < \alpha_{02} < \alpha_{03}$, where the two extreme values represent unstable equilibrium interface shapes and the middle one corresponds to a stable configuration; in the latter case, the stable solution of (28) is, in a first approximation,

$$\alpha_0 = -\beta_0. \tag{31}$$

Eq. (29) and (30) allow one to calculate the self-similar transfer function $\Phi(\Omega) = 1/2\ \lambda\ F(\omega)$, as well as the phase-difference

$$\Phi(\Omega) = \alpha/\beta = [\gamma^2\Omega^2 + (\Omega^2 + 3\alpha_0^2 - 1)^2]^{-1/2} \tag{32}$$

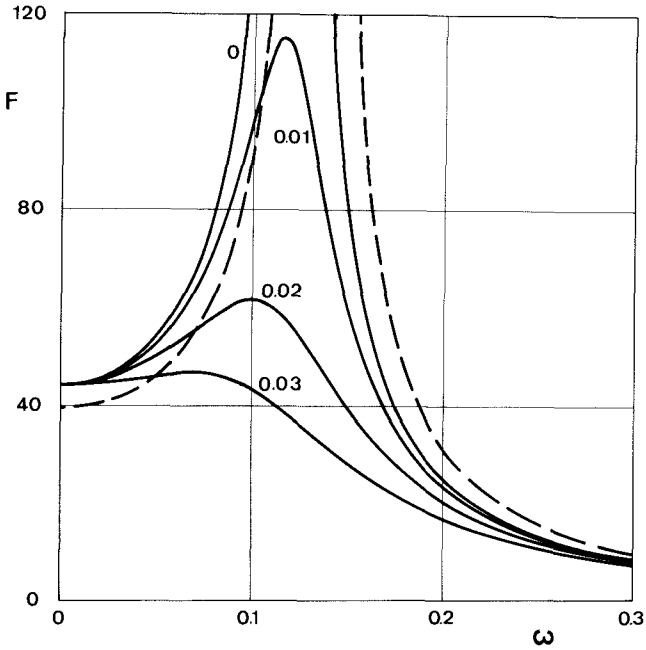

Fig. 4. Transfer function $F(\omega)$, defined by eq. (21) or (37), of liquid bridges between equal disks ($K = 1$), slenderness $\Lambda = 3$ and cylindrical volume ($V = 2\pi\Lambda$) in gravitationless conditions ($B = 0$). Dashed line corresponds to results obtained through slice model whereas continuous lines correspond to the self-similar one. Numbers on the curves indicate the value of the viscous to capillary forces ratio C

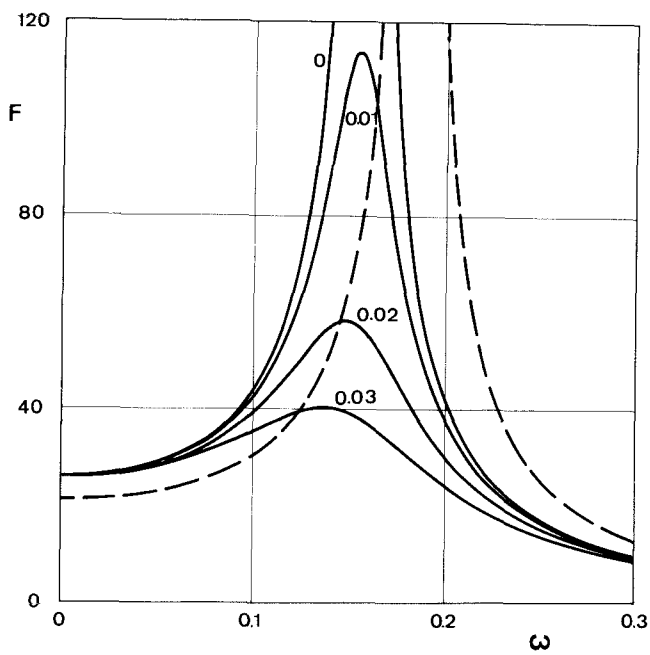

Fig. 5. Transfer function $F(\omega)$, defined by eq. (21) or (37), of liquid bridges between equal disks ($K = 1$), slenderness $L = 2.9$ and cylindrical volume ($V = 2\pi\Lambda$) in gravitationless conditions ($B = 0$). Dashed line corresponds to results obtained through slice model whereas continuous lines correspond to the self-similar one. Numbers on the curves indicate the value of the viscous to capillary forces ratio C

$$\tan\varphi = \gamma\Omega/(\Omega^2 + 3\,\alpha_0^2 - 1) \tag{33}$$

The pulsation of resonance, Ω_r, results from (32); the values of Ω for which $\Phi(\Omega)$ is maximum are

$$\Omega_r = \left(1 - 3\,\alpha_0^2 - \frac{1}{2}\,\gamma^2\right)^{1/2} \approx \left(1 - 3\,\beta_0^2 - \frac{1}{2}\,\gamma^2\right)^{1/2} \tag{34}$$

where the second of expressions (34) has been written taking into account (31). Therefore, in dimensionless physical variables, the resonance pulsation, phase difference at resonance and transfer function are

$$\omega_r = \frac{2}{5}\,(2\,\lambda)^{1/2}\left(1 - \frac{9}{4}\,\frac{B^2}{\lambda^3} - \frac{25}{16}\,\frac{C^2}{\lambda^2}\right)^{1/2} \tag{35}$$

$$\tan\varphi_r = -\frac{8}{5}\,\frac{\lambda}{C^2}\,\omega_r \tag{36}$$

$$F(\omega) = \frac{2}{\lambda}\left[1 - \frac{9}{4}\,\frac{B^2}{\lambda^3} + \frac{625}{64}\,\frac{\omega^2\,(\omega^2 - 2\,\omega_r^2)}{\lambda^2}\right]^{-1/2} \tag{37}$$

Note that in these expressions B means the static Bond number associated to the mean value of microgravity. It must be pointed out that if unequal disks were considered ($K \neq 1$) all the mathematical considerations reported in [17] would be applicable to the unequal-disk case by using $B - H/2\,\pi$ instead of B ([13]). In such a case the present reasoning would be valid for the unequal-disk case if in (26) β_0 accounts for both mean gravity and unequal disks effects, and $\varepsilon\beta\cos(\Omega\theta - \varphi)$ accounts only for time variation of gravity. Then, eq. (35) - (37) would be valid for the unequal-disk case if $B - H/2\,\pi$ is considered instead of B.

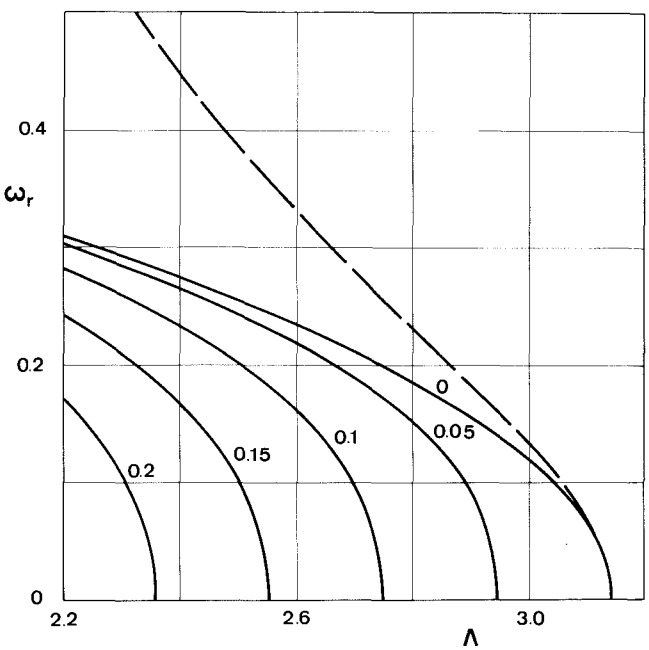

Fig. 6. Variation with the slenderness Λ of the pulsation of resonance ω_r of cylindrical volume liquid bridges between equal disks in gravitationless conditions ($V = 2\pi\Lambda$, $K = 1$, $B = 0$). Dashed line corresponds to results obtained through slice model whereas continuous lines correspond to the self-similar one. Numbers on the curves indicate the value of the viscous to capillary forces ratio C

The transfer function $F(\omega)$ as given by eq. (37) has been represented in figs. 4 and 5 for liquid bridges between equal disks having slendernesses $\Lambda = 3$ and $\Lambda = 2.9$, respectively. In both cases the liquid volume is the cylindrical one ($V =$

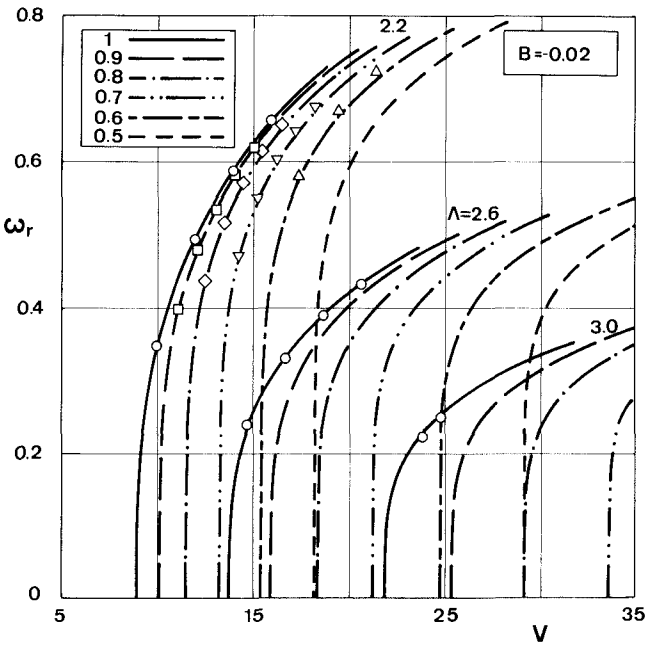

Fig. 7. Variation of the pulsation of resonance corresponding to the first mode ω_r with the liquid bridge volume, V, the slenderness, Λ, and the disks radius ratio, K. The results correspond to a mean axial gravity level B = −0.02. Symbols indicate numerical results whereas lines correspond to results obtained by using eq. (38). The line type indicates, according to the insert, the value of the disks radius ratio K

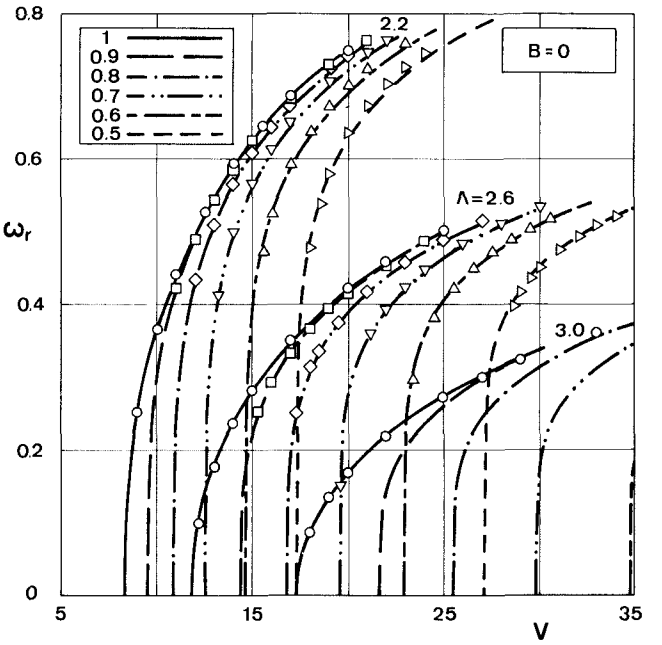

Fig. 8. Variation of the pulsation of resonance corresponding to the first mode ω_r with the liquid bridge volume, V, the slenderness, Λ, and the disks radius ratio, K. The results correspond to a mean axial gravity level B = 0. Symbols indicate numerical results whereas lines correspond to results obtained by using eq. (38). The line type indicates, according to the insert, the value of the disks radius ratio K

$2\pi\Lambda$) and $B = 0$. These plots show the influence of viscosity on the dynamic response of the liquid bridge: as viscosity increases, the maximum of $F(\omega)$ corresponding to the first mode decreases and the resonance pulsation diminishes. In these plots, the transfer function, $F(\omega)$, corresponding to the one-dimensional inviscid slice model has been also plotted.

The influence of viscosity on the pulsation of resonance is clearly seen in fig. 6, where the variation of ω_r with Λ, for the case of liquid bridges with $K = 1$, $B = 0$ and $V = 2\pi\Lambda$ is shown. As it can be observed by comparing the two curves corresponding to inviscid liquid bridges, the self-similar model fails when the liquid bridge configuration is far from the reference configuration ($\Lambda \approx \pi$, $V \approx 2\pi\Lambda$, $K \approx 1$ and $B \approx 0$).

3.3 Resonance Frequencies

Finally, in addition to the analytical methods presented in sections 3.1 and 3.2, the numerical method described in [16] (which is a generalization to $B \neq 0$ and $K \neq 1$ of that introduced in section 3.1) has been used to calculate resonance pulsations ω_r of general liquid bridge configurations. These numerical data have been used to fit a mathematical expression which gives the dependence on Λ, V, B and K of ω_r. It is out of the scope of this paper to present detailed information on the fitting process which, because of the large number of parameters involved (Λ, V, B, K), required some amount of intuition. The resulting equation for ω_r, using dimensionless variables, is

$$\omega_r = E_0(V - V_m)^M + E_1(V - V_m)^{(\Lambda+3)M} \qquad (38)$$

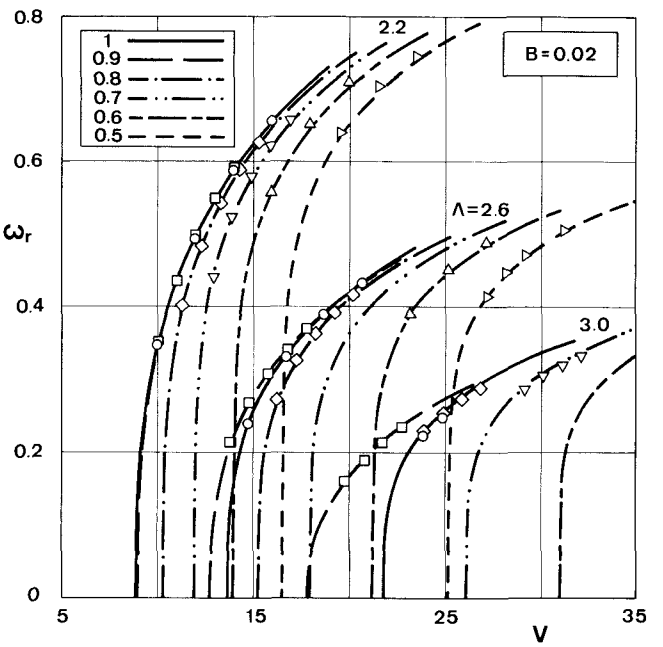

Fig. 9. Variation of the pulsation of resonance corresponding to the first mode ω_r with the liquid bridge volume, V, the slenderness, Λ, and the disks radius ratio, K. The results correspond to a mean axial gravity level B = 0.02. Symbols indicate numerical results whereas lines correspond to results obtained by using eq. (38). The line type indicates, according to the insert, the value of the disks radius ratio K

where V is the volume of the liquid bridge, $V_m = V_m(\Lambda, K, B)$ is the minimum volume stability limit as given by eq. (3), and E_0, M and E_1 depend on Λ and the parameter D (see eq. (2)) as follows

$$E_0 = 4.3151\,\Lambda^{-3.39}\,(1 + 0.2063\,D\Lambda^{6.1349})^{1/4} \tag{39}$$

$$M = (0.17 + 0.105\,\Lambda)\,[1 + D(\Lambda - 0.5)^{4.778}]^{-1/\Lambda} \tag{40}$$

$$\begin{aligned} E_1 = {} & 10^{-5}\,[0.5076 - 5\,(\Lambda - 1.62)^{-3}] \\ & - 10^{-3}\,[1.381 + 3.8\,(\Lambda - 1.4)^{-2.5}]\,D \\ & + 10^{-1}\,(1.5 - \Lambda)\,D^2\,(D - 0.4) \\ & + (0.0324 - 0.018\,\Lambda)\,D\{[1 + (60\,D)^3]\Lambda\}^{-1} \end{aligned} \tag{41}$$

Eq. (38) is valid, at least, in the range $0 \leq V - V_m \leq 10$, $2 \leq \Lambda \leq 3.2$, $0.5 \leq K \leq 1$ and $|B| \leq 0.05$. To get an idea on the accuracy of (38) this expression is compared with numerical data in figs. 7 to 9. Each of these plots shows the variation with V, Λ and K of ω_r for three different values of the Bond number B. As it can be observed, the agreement between eq. (38) and the numerical data is good and the discrepancies between (38) and the numerical data increase as K decreases.

4 Conclusions

Analytical expressions for the variation with the slenderness Λ, disks radius ratio K, and Bond number B of the minimum-volume stability limit V_m and for the dependence with Λ, K, B, and the volume of the liquid bridge V (formally $V - V_m$) of the pulsation of resonance of long axisymmetric liquid bridges have been obtained. Both expressions allow one, within their ranges of application, to get in simple equations information which up to now was only partially available in graphical and/or numerical form, and dispersed over several publications.

In addition, the dynamic response of long liquid bridges in a time-dependent axial microgravity field has been analytically calculated by using two different mathematical one-dimensional models, one of them including viscosity effects.

All these results are useful in designing liquid bridge experiments because they provide simple mathematical tools which could be implemented in checking and/or control devices.

Acknowledgement

This work has been supported by the Spanish Comisión Interministerial de Ciencia y Tecnologia (CICYT) and is part of a more general endeavour for the study of fluid physics and materials processing under microgravity (Project No. ESP 88-0359).

References

1 *Wilcox, W. R.*, in: Encyclopedia of Chemical Technology, Vol. 24, John Wiley & Sons, Inc., p. 903/917 (1984).
2 LEYBOLD-HERAEUS GmbH, Floating Zone Melting of Refractory Metal Rods, Leybold-Heraeus GmbH, Bonner Straße 504, D-5000 Köln, FRG, 1977.
3 *Eyer, A.; Leiste, H.; Nitsche, R.*: in: ESA SP-222, ESA, Paris, p. 173/182 (1984).
4 *Eyer, A.; Leiste, H.; Nitsche, R.*: J. Crystal Growth 71, 173 (1985).
5 *Martínez, J.*, in: ESA SP-222, ESA, Paris, p. 31/36 (1984).
6 *Martínez, I.; Meseguer, J.*, in: Scientific Results of the German Spacelab Mission D1, Sahm, P. R., Jansen, R., Keller, M. H. (Eds.), DVFLR, Köln, FRG, p. 105/112 (1987).
7 *Martínez, I.; Sanz, A.*: ESA Journal 9, 323 (1985).
8 *Meseguer, J.; Sanz, A.*: J. Fluid Mech. 153, 83 (1985).
9 *Vega, J. M.; Perales, J. M.*, in: ESA SP-191, ESA, Paris, p. 247/252 (1983).
10 *Meseguer, J.*, in: ESA SP-222, ESA, Paris, p. 297/300 (1984).
11 *Meseguer, J.; Mayo, L. A.; Llorente, J. C.; Fernández, A.*: J. Crystal Growth 73, 609 (1985).
12 *Perales, J. M.*: Acta Astronautica 15, 561 (1987).
13 *Meseguer, J.*: J. Crystal Growth 67, 141 (1984).
14 *Meseguer, J.*: J. Crystal Growth 73, 599 (1985).
15 *Martínez, I.; Perales, J. M.*: J. Crystal Growth 78, 369 (1986).
16 *Meseguer, J.*: Appl. Microgravity Tech. 1, 136 (1988).
17 *Rivas, D.; Meseguer, J.*: J. Fluid Mech. 138, 417 (1984).
18 *Meseguer, J.*: J. Fluid Mech. 130, 123 (1983).
19 *Meseguer, J.*: J. Crystal Growth 62, 577 (1983).
20 *Green, A. E.*: Int. J. Engng. Sci. 14, 49 (1976).
21 *Bogy, D. B.*: Phys. Fluids 21, 190 (1978).
22 *Bogy, D. B.*: Ann. Rev. Fluid Mech. 11, 207 (1979).
23 *Stoker, J. J.*: Nonlinear Vibrations in Mechanical and Electrical Systems, Interscience Publishers, New York, London, Sydney, 1966.

List of Symbols

B	Gravity to capillary forces ratio, Bond number, $B = \varrho\, g\, R_0^2/\sigma$
C	Viscous to capillary forces ratio, $C = \nu\,(\varrho/\sigma\, R_0)^{1/2}$
D	Non-symmetric effect parameter, defined by equ. (2)
$F(\omega)$	Dimensionless transfer function, made dimensionless with $\sigma/\varrho\, R_0^4$
H	Unequal disks parameter, $H = (1-K)/(1+K)$
K	Small to large disk radius ratio, $K = R_1/R_2$
L	Liquid bridge length, [m]
$P(z,t)$	Dimensionless reduced pressure, made dimensionless with $\sigma/\varrho\, R_0$
$Q(z,t)$	Dimensionless axial momentum, $Q(z,t) = S(z,t)\, W(z,t)$, made dimensionless with $(\sigma\, R_0^3/\varrho)^{1/2}$
$R(z,t)$	Dimensionless interface radius, made dimensionless with R_0
R_0	Mean radius of the liquid bridge, $R_0 = (R_1 + R_2)/2$, [m]
R_1, R_2	Radius of the disks, [m]
$S(z,t)$	Dimensionless cross-section area, $S(z,t) = [R(z,t)]^2$, made dimensionless with R_0^2
V	Dimensionless volume of liquid, made dimensionless with R_0^3
$V_m(\Lambda, K, B)$	Dimensionless minimum-volume stability limit, made dimensionless with R_0^3
$W(z,t)$	Dimensionless axial velocity, made dimensionless with $(\sigma/\varrho\, R_0)^{1/2}$
g	Microgravity acceleration, [m s^{-2}]
r, z	Dimensionless coordinates, made dimensionless with R_0
t	Dimensionless time, made dimensionless with $(\varrho\, R_0^3/\sigma)^{1/2}$
Λ	Liquid bridge slenderness, $\Lambda = L/(R_1 + R_2)$
φ	Phase difference, [rad]
$\omega(\Lambda, K, B)$	Dimensionless pulsation, equal to $2\,\pi$ times the frequency, made dimensionless with $(\varrho\, R_0^3/\sigma)^{-1/2}$
ϱ	Liquid density, [kg m^{-3}]
σ	Surface tension, [N m^{-1}]
ν	Kinematic viscosity [m^2 s^{-1}]

Subscripts

r	Indicate values at resonance

Other symbols, when required, are defined in the text.